

RESEARCH ARTICLE

Novel approach for predicting the creep behavior of ceramic fibers using dimensional analysis

Renan Belli Berman¹ | Renato Saint Martin Almeida²  | Mohamed Ariff Azmah Hanim³ | Edson Roberto de Pieri⁴ | Hazim Ali Al-Qureshi¹

¹Department of Mechanical Engineering, Federal University of Santa Catarina (UFSC), Joinville, Brazil

²Advanced Ceramics, University of Bremen, Bremen, Germany

³Department of Mechanical and Manufacturing Engineering, University Putra Malaysia, Serdang, Malaysia

⁴Department of Automation and Systems Engineering, Federal University of Santa Catarina (UFSC), Florianópolis, Brazil

Correspondence

Renato Saint Martin Almeida, Advanced Ceramics, University of Bremen, Bremen 28359, Germany.

Email: renato.almeida@uni-bremen.de

Abstract

A more generalized approach for predicting the steady-state creep rate of ceramic fibers under extensive stress ranges is proposed. Creep rate equations derived from dimensional analysis, such as Almeida's creep equation and Arrhenius' creep equation, were evaluated using Buckingham's method, and the corresponding π groups were determined. Subsequently, a new equation is proposed using the usual semi-empirical constants for the diffusional and power law creep phenomena, along with an additional power law exponent to account for changes in creep mechanisms at higher stresses. The proposed equation was used to fit the creep rate data of the fiber Nextel 720 at various temperatures and constant stress, which demonstrated a good fit with an adjusted R-squared of .96. Subsequently, the equation was used to predict the creep rate at constant temperature and various stresses, exhibiting an adjusted R-squared of .77 and .85, depending on the scatter of the used data. The predictive results of the proposed equation were then compared to those obtained using the Arrhenius creep equation, which tends to higher rates at high stresses. In summary, the novel equation can be more efficiently applied in predicting the creep rate of ceramic fibers across a broader spectrum of stress.

KEYWORDS

creep, dimensional analysis, fibers, mullite

1 | INTRODUCTION

Ceramic matrix composites (CMCs) have gained space in several advanced applications such as aircraft turbine engine components, heat shielding of space vehicles, hypersonic flight vehicles and devices, as well as hot gas filters. These applications demand structural components that exhibit high strength, as well as thermal and chemical stability under various environments.¹ CMCs maintain excellent strength even at high temperatures, making their

creep behavior a crucial factor for their selection. Among these composites, the use of oxide CMCs has increased over the last decades due to their higher chemical stability when compared to non-oxide CMCs, especially for applications in oxidizing atmospheres.² Hence, the creep behavior of oxide CMCs has been extensively studied by several authors.^{3–5}

Oxide fibers are known for exhibiting lower creep resistance compared to non-oxide materials. When assessing composite materials loaded in the direction of the fibers,

This is an open access article under the terms of the [Creative Commons Attribution](https://creativecommons.org/licenses/by/4.0/) License, which permits use, distribution and reproduction in any medium, provided the original work is properly cited.

© 2024 The Author(s). *International Journal of Applied Ceramic Technology* published by Wiley Periodicals LLC on behalf of American Ceramics Society.

the predominant factor influencing creep resistance is the creep resistance of the fibers.⁶ Consequently, the performance of commercially available fibers has become a focal point in the literature, as evidenced by several studies.^{7–9} The primary objective of these works was to ascertain the steady-state creep rate under varying test conditions. The results were then fitted using established creep equations and models originally designed for bulk ceramics and other materials. Frequently, the relation following the Arrhenius rate equation or its power law equivalent is employed for this purpose. However, it is worth noting that while these equations can be used to fit the available data, they pose challenges when used for predicting creep rates under diverse conditions due to the inherent complexity in accurately measuring certain material constants and properties required by these equations.¹⁰ Furthermore, none of the commonly used equations can accommodate the creep rate across a wide range of temperature or stress values, nor do they directly address the material's anticipated behavior under both lower and higher stress conditions concurrently. For instance, it has been reported that the mullite fiber Nextel 720 shows a shift in stress exponent when tested under stresses higher than 300 MPa at 1200°C.¹¹ This change of stress exponent is associated with changes in the main creep deformation mechanisms, which cannot be predicted with the Arrhenius creep rate equation.

Other methods for predicting the effects of mechanical stress on materials at high temperatures are documented in the literature. However, they also present significant challenges. For instance, thermo-mechanical simulations can yield highly accurate predictions regarding the effects of both temperature and stress.^{12–14} Nonetheless, a comprehensive model of the material's characteristics and behavior under the specified simulation conditions is required to perform such simulations. This is particularly challenging for novel materials such as ceramic fibers, as many of their properties are difficult or costly to test. The use of machine learning algorithms to create predictive curves or equations is also gaining significant attention in the literature. This trend is attributed to the large array of available algorithms, which are tailored to the complexity of the dataset; not to mention that they can effectively process a large volume of data.^{15–17} One significant drawback of machine learning algorithms is that their predicted equations lack physical correlation. Consequently, complex physical phenomena such as creep in ceramic fibers can easily lead to erroneous predictions or result in overfitting, in which the generated curves are strongly associated with the specific dataset rather than generalizing accurately across different conditions.

The present work addresses the theoretical formulation of the creep of ceramic fibers using dimensional analysis. The main aim is to formulate a novel equation that

can predict the steady-state creep rate of ceramic fibers in a wide stress range. For that, Almeida's general parameters for dimensional analysis¹⁰ are used together with the introduction of an additional stress exponent to account for the creep rate at higher applied stresses. Additionally, the Arrhenius creep rate equation is derived through dimensional analysis to exemplify the distinct general parameters used in dimensional analysis. A comparative analysis is subsequently conducted between the theoretical framework and experimental results, allowing for the evaluation of the predictive capabilities of each equation.

2 | DIMENSIONAL ANALYSIS

Dimensional analysis is a procedure algebraically formalized by Buckingham to analyze and describe any physical process or state.¹⁸ This procedure involves analyzing the variables and constants of a problem in relation to their fundamental dimensions to obtain a complete set of independent dimensionless products. This allows us to produce a dimensionally homogeneous equation. To apply dimensional analysis to the creep of ceramic fibers, the main variables and constants that relate to the problem must be listed and their basic dimensions evaluated.

In the paper published by Almeida, et al.¹⁰ their proposed equation presents a good fit to the experimental data, while simultaneously offering much simpler variables to measure and control compared to the Arrhenius creep rate equation and the power law equivalents. The main parameters chosen by Almeida for the dimensional analysis, along with their SI units, are shown in Table 1.

Where σ is the stress applied to the fiber, G is the fibers shear modulus, θ is the temperature, θ_0 is a temperature constant to account for temperature changes, Q is the creep activation energy, R is the gas constant, b is the burgers vector, d is the grain size of the fiber, D_0 is a diffusion constant, and $\dot{\epsilon}$ is the creep rate. As for the dimensions: M is mass, L is space, T is time, θ is temperature, and N is the number of mols.

To find the relation between the variables, the dimensionless products (or π products) must be evaluated. The Buckingham π theorem states that the number of dimensional products (N_p) is equal to the number of variables and constants that describe the problem (N_v) minus the number of dimensions needed to express their dimensional formulae (N_d).^{19,20} This relationship is expressed in Equation (1):

$$N_p = N_v - N_d \quad (1)$$

In this case, the number of variables (N_v) is 10 and the number of dimensions (N_d) is 5. Consequently, the number

TABLE 1 Main parameters chosen and their SI units.

Variable name	Variable symbol	SI units	Dimensions
Stress applied to the fiber	$[\sigma]$	$kg^1m^{-1}s^{-2}$	$ML^{-1}T^{-2}$
Fiber's shear modulus	$[G]$	$kg^1m^{-1}s^{-2}$	$ML^{-1}T^{-2}$
Temperature	$[\theta]$	K^1	θ^1
Temperature constant to account for temperature changes	$[\theta_0]$	K^1	θ^1
Activation energy of the creep	$[Q]$	$kg^1m^2s^{-2}K^{-1}$	$ML^2T^{-2}N^{-1}$
Gas constant	$[R]$	$kg^1m^2s^{-2}K^{-1}mol^{-1}$	$ML^2T^{-2}\theta^{-1}N^{-1}$
Burgers vector	$[b]$	m^1	L
Grain size of the fiber	$[d]$	m^1	L
Diffusion constant	$[D_0]$	m^2s^{-1}	L^2T^{-1}
Creep rate	$[\dot{\epsilon}]$	s^{-1}	T^{-1}

	ϵ	σ	Q	$\theta\theta$	d	R	θ	G	b	D_0
M	0	1	1	0	0	1	0	1	0	0
L	0	-1	2	0	1	2	0	-1	1	2
T	-1	-2	-2	0	0	-2	0	-2	0	-1
θ	0	0	0	1	0	-1	1	0	0	0
N	0	0	-1	0	0	-1	0	0	0	0

FIGURE 1 Matrix MT where the first five columns are matrix and the final five columns (in blue) are matrix A and B .

	ϵ	σ	Q	$\theta\theta$	d	R	θ	G	b	D_0
π_1	1	0	0	0	0	0	0	0	2	-1
π_2	0	1	0	0	0	0	0	-1	0	0
π_3	0	0	1	0	0	-1	-1	0	0	0
π_4	0	0	0	1	0	0	-1	0	0	0
π_5	0	0	0	0	1	0	0	0	-1	0

FIGURE 2 π group matrix.

of dimensionless products equals five. These dimensionless products can be determined using linear algebra, in a process known as modern dimensionless analysis.^{19,21} This method requires a matrix MT with rows representing the variables and columns representing the dimensions of the problem. Subsequently, matrix MT is subdivided into two matrices, A and B . Matrix A has the same number of rows as the dimensions of the problem and a nonzero determinant, while matrix B is composed of the remaining variables. In this specific case, the number of rows is identical for matrices A and B . The matrix MT for the creep problem is represented in Figure 1.

The resulting π groups can be determined by a matrix composed of an identity matrix of the same size as matrix B , and a matrix composed of the negative transpose of the inverse of matrix A multiplied by matrix B .^{19,21} Referred to as the π group matrix, each line in this matrix corresponds to a distinct π group of the problem, illustrated in Figure 2.

Hence, the π groups of this problem are determined by evaluating each line of the matrix as an exponent in their respective variables, as listed in Equation (2):

$$\begin{aligned}\pi_1 &= \dot{\epsilon}b^2D_0^{-1}, \quad \pi_2 = \sigma G^{-1}, \quad \pi_3 = QR^{-1}\theta^{-1}, \\ \pi_4 &= \theta\theta_0^{-1}, \quad \pi_5 = db^{-1}\end{aligned}\quad (2)$$

To obtain the proposed equation for creep, the fundamental equation of Buckingham π theorem represented by Equation (3) is stated:

$$\varphi(\pi_1, \pi_2, \pi_3, \pi_4, \pi_5) = 0 \quad (3)$$

From the fundamental equation of the Buckingham π theorem, each dimensionless variable can be manipulated by a mathematical function while preserving its dimensionless nature.^{18,19,22} Thus, Equation (4) is obtained by

applying the exponential function to π_3 , the power function to π_2 with exponents n and m , and π_5 with the negative exponent p from Equation (3):

$$\varphi(\pi_1, \pi_2^{nm}, \exp(1/\pi_3), \pi_4, \pi_5^{-p}) = 0 \quad (4)$$

The grain size exponent p is associated with diffusional creep. A p exponent of 2 corresponds to the Nabarro–Herring model, that is, diffusion primarily through volumetric diffusion inside the grains.² A p exponent of 3 corresponds to the Coble model, indicative of diffusion through grain boundaries.^{8,10,23} The stress exponent n can be related to multiple creep mechanisms depending on the temperature and stress ranges, but can be abstracted as the usual power law creep exponent for low stresses. As previously mentioned, the main problem on the determination of n lies on the fact that different creep mechanisms can take place at different stress ranges. Thus, the power law creep exponent can be divided into different exponents. Hence, it is proposed here the inclusion of another exponent m , which accounts for changes in the creep deformation that are stress sensitive. In the case described above, the n exponent behaves akin to the power law creep exponent and can be determined through fitting to experimental data, with the m exponent equaling one in this scenario. Conversely, for high stresses, the n exponent retains its value from the low-stress creep mechanism, while the m exponent is fitted to the new experimental data. This approach allows for the simultaneous visualization of both low- and high-stress mechanisms in the equation. There are other equations in the literature that utilize a m exponent for creep, such as the Dorn and the Norton creep equations.²⁴ However, the m exponent has no generalized meaning, contrasting with the n exponent which is generally used as the power law exponent or the p exponent which is used as the diffusional exponent.¹

Equation (5) is obtained by applying properties of multivariable functions to Equation (4):

$$\dot{\epsilon} b^2 D_0^{-1} = \left(\frac{\sigma}{G}\right)^{nm} \left(\frac{\theta}{\theta_0}\right) \left(\frac{d}{b}\right)^{-p} \exp\left(\frac{R\theta}{Q}\right) \quad (5)$$

Equation (6) is obtained by simple manipulation of the variables of Equation (5):

$$\dot{\epsilon} = \frac{D_0 b^{p-2} \sigma^{nm} \theta}{G^{nm} d^p \theta_0} \exp\left(\frac{R\theta}{Q}\right) \quad (6)$$

To simplify the equation, two constants are defined: constant C is an activation energy constant equal to R/Q and k

is a material constant shown in Equation (7):

$$k = \frac{D_0 b^{p-2}}{\theta_0 G^{nm}} \quad (7)$$

Substituting the defined constants in Equation (6), we obtain the proposed general equation for the creep of ceramic fibers:

$$\dot{\epsilon} = k \frac{\sigma^{nm} \theta}{d^p} \exp(C\theta) \quad (8)$$

The proposed equation shows that the creep rate is proportional to the material constants (k and C), to the stress and to the temperature, while being inversely proportional to the grain size of the material. These findings are supported by other studies in ceramic fibers.^{25–28} Furthermore, Almeida's equation for the creep of ceramic fibers is a specific form of the proposed equation finely tuned to the creep of oxide ceramic fibers, where nm and p are both equal to 3 as shown in Equation (9):

$$\dot{\epsilon}_{Almeida} = k \frac{\sigma^3 \theta}{d^3} \exp(C\theta) \quad (9)$$

The Arrhenius equation for creep can also be derived through dimensional analysis. The chosen variables are the same as Almeida's, with the exception of removing θ_0 and adding the Boltzmann constant (k_b). Since the number of variables and dimensions remains unchanged from the previous analysis, it will yield the same number of dimensionless products. By repeating the linear algebra procedure with the modified variables, the only π group to differ will be the group containing the Boltzmann constant, as represented in Equation (10). The remaining π groups will be the same as the ones previously found.

$$\pi_4 = \frac{k_b \theta}{G b^3} \quad (10)$$

From the fundamental equation of the Buckingham π theorem, Equation (11) is obtained by applying the exponential function on π_3 and the power function on π_2 and π_5 :

$$\varphi(\pi_1, \pi_2^n, \exp(-\pi_3), \pi_4^{-1}, \pi_5^{-p}) = 0 \quad (11)$$

Equation (12) is obtained by applying properties of multivariable functions to Equation (11):

$$\dot{\epsilon} b^2 D_0^{-1} = A \frac{G b^3}{k_b \theta} \left(\frac{\sigma}{G}\right)^n \left(\frac{d}{b}\right)^{-p} \quad (12)$$

Equation (13) is obtained by simple manipulation of the variables of Equation (12):

$$\dot{\epsilon} = Ab^{-2}D_0 \frac{Gb^3}{k_b\theta} \left(\frac{\sigma}{G}\right)^n \left(\frac{d}{b}\right)^{-p} \exp\left(\frac{-Q}{R\theta}\right) \quad (13)$$

Equation (14) is the definition of diffusion:

$$D = D_0 \exp\left(\frac{-Q}{R\theta}\right) \quad (14)$$

Equation (15) is the Arrhenius equation for creep and is obtained by substituting Equation (14) on Equation (13):

$$\dot{\epsilon}_{Arrhenius} = A \frac{D G b}{k_b \theta} \left(\frac{\sigma}{G}\right)^n \left(\frac{b}{d}\right)^p \quad (15)$$

3 | DISCUSSION OF RESULTS AND DATA FITTING

The investigations on creep conducted in this study utilized the mullite fiber from Nextel 720, Lot. 10015, manufactured by 3 M corporation.²⁹ The fibers were extracted from a 3000 denier bundle, which corresponds to 750 fiber filaments per bundle. Each filament has a diameter ranging from 10 to 12 μm . Nextel 720 is composed of several misoriented mullite grains forming 500 nm mullite mosaics with smaller α -alumina grains interspersed.⁸ To access the performance of the fibers under the application conditions of oxide CMCs, tensile creep tests were conducted on single filaments. The creep tests were performed according to the standard DIN EN 15365.³⁰ In this procedure, the upper end of a single filament was attached to the testing equipment, while the lower end of the filament was affixed to a weight applying constant load during the creep test. An oven then heated the sample at a rate of 1 K/s to the target temperature. Finally, a capacitive noncontact displacement transducer recorded the displacement of the specimen. The specimens were tested until failure, or until a run-out time of 50 h was achieved. An image of the testing apparatus with the sample is shown in Figure 3.²⁹

With the creep data of Nextel 720, conducted at temperatures ranging from 1373 to 1573 K with a constant creep stress of 150 MPa, and knowing the initial grain size of the fiber, the values of the constants k , n , and C can be determined by data fitting. Given that the constant stress falls within the low-stress range for this fiber type, the constant m is fixed at 1. Initially, constant n is assigned a value of 3, a recognized power law creep exponent in the literature for this fiber under such stress and temperature range.^{8,10,11,23} However, additional values within the range of 1–7 are also examined to determine the optimal fit.

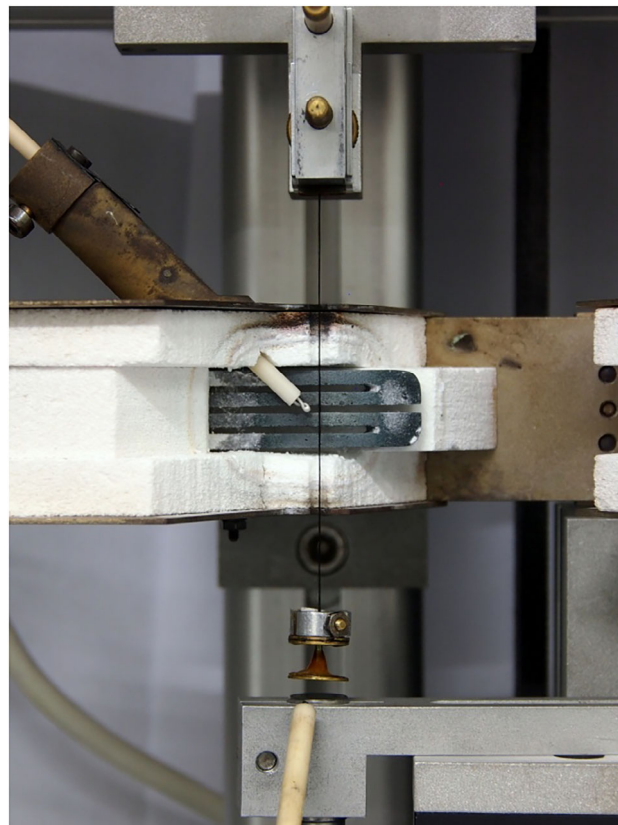


FIGURE 3 Creep testing apparatus.²⁹

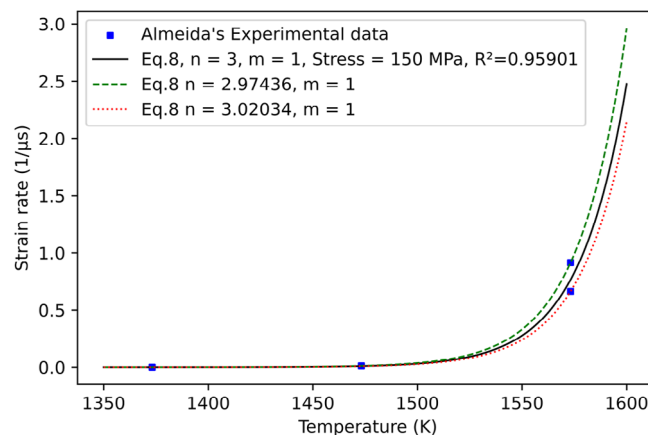


FIGURE 4 Best fit of creep rate for constant 150 MPa stress by the proposed equation.

The value obtained for k is $1.81 \cdot 10^{-39} \text{ nm}^3 / (\text{MPa}^3 \cdot \text{K} \cdot \text{s})$ and the value obtained for C is $.0432 \text{ K}^{-1}$, which correspond to the values found by Almeida, et al.¹⁰ With these values, the upper and lower limits of the values of n for the experimental data are also determined, as shown in Figure 4.

By utilizing the constants derived from the creep test under a constant stress of 150 MPa, the proposed equation can be easily used to predict values at different stresses and

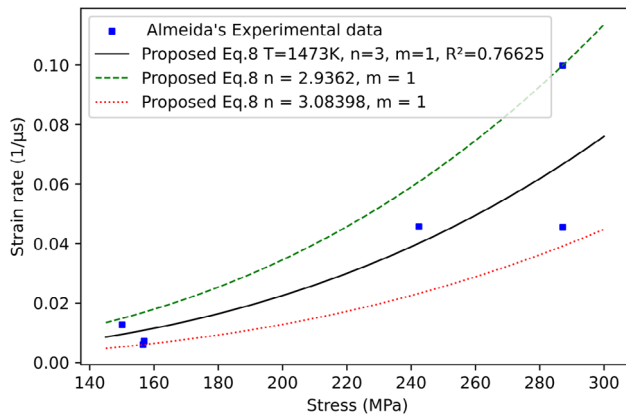


FIGURE 5 Prediction of creep rate for constant 1473 K temperature by the proposed equation.

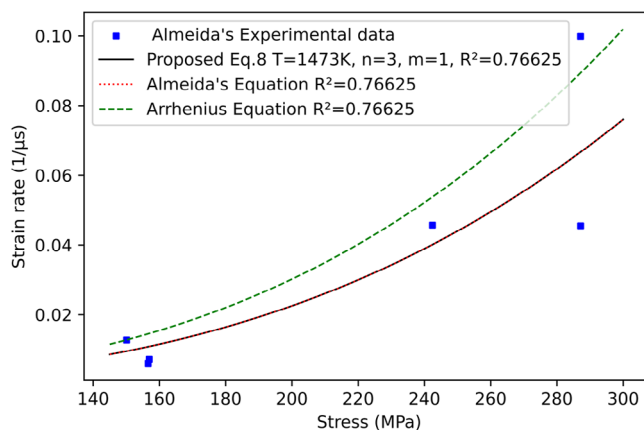


FIGURE 6 Almeida's and Arrhenius prediction of the creep data for constant 1473 K temperature.

at a constant temperature. The creep rate of Nextel 720 at constant 1473 K and different stresses of 100–300 MPa were calculated using the proposed equation and compared to the experimental creep data under the same conditions as shown in Figure 5. The proposed equation facilitates the observation of limit values for the power law creep. Notably, a more substantial variation in the n values is observed at a constant temperature with varying stress levels, as compared to the constant low-stress creep under different temperatures depicted in Figure 4.

Figure 6 illustrates a comparison between the proposed equation with the Arrhenius and Almeida's equations for fitting the same data. The three equations present an equally good fit for the given experimental data, with all equations presenting an R^2 value of .95902 for the creep tests under constant 150 MPa stress, and an R^2 value of .76625 for the creep tests at constant 1473 K. Although the Arrhenius and Almeida's equations exhibit similar R^2 values, it can be observed that the Arrhenius equation consistently predicts higher values when compared to either Almeida's or the proposed equation of this work.

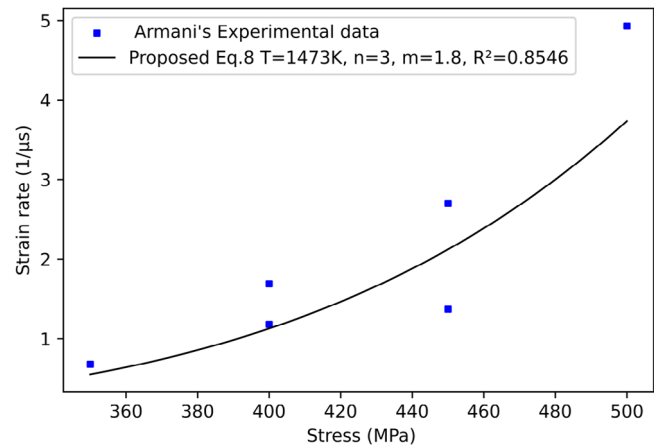


FIGURE 7 Best fit of the creep rate by the proposed equation for Armani's experimental creep data at constant 1373 K temperature.^{1,11}

In assessing the proposed m exponent for creep of Nextel 720 in high-stress ranges, supplementary data from the literature for the same fiber were used.^{1,11} The constants C and n remain consistent with those obtained from the previous experimental data, given the identical fiber composition. The exponent value m and the constant k of Equation (8) are evaluated by best fit for the creep data presented by Armani for the creep of Nextel 720 fibers at constant 1475 K and multiple stresses (Figure 7). The k constant had to be recalibrated for high stresses due to its inherent dependence on the constant m as can be seen in Equation (7). The optimal fit yields an m exponent value of 1.8, a k constant of $7.618 \cdot 10^{-45} \frac{nm^3}{MPa^3 \cdot K \cdot s}$, with an R^2 value of .8546. Multiplying the obtained m exponent with the previously obtained n exponent results in a value of 5.4, closely approximating the literature's power law equivalent exponent of 5 for this fiber at the specified temperature and stress range.¹¹ As seen in Figure 7, the proposed equation can more generally describe the steady-state creep rate, even at very different stress ranges. Studies using other power-law creep equations often cannot describe the creep rate over extensive stress ranges.^{8,10,11} Compared to the fit using Almeida's experimental data at constant temperature (Figure 6), it can be seen that the R^2 value is higher with Armani's data (Figure 7). This can be related to the smaller scatter in the cited data. Significant data scatter is a common occurrence during the mechanical characterization of ceramic fibers. This goes by the fact that fiber handling and testing is a difficult task, which can end up influencing the results. Furthermore, variance between tested fibers can also lead to high scatter within measurements.³¹ This further highlights the importance of formulating a creep rate equation that can correctly predict the data.

4 | CONCLUSIONS

Using dimensional analysis, a novel semi-empirical equation for the steady-state creep rate of ceramic fibers was proposed. Furthermore, Arrhenius and Almeida's equations for creep could also be derived by dimensional analysis. The equation proved to be a useful tool to identify the relationship between the variables related to the creep of ceramic fibers. The exponent m of the proposed equation presents an easier method of evaluating the stress exponent at higher stresses. While the exponent n can be determined under a short range of stresses and constant temperature, the value of m can be evaluated for other stress ranges. This allows the equation to directly represent the main creep mechanism active in each stress range, unlike other approaches.

The proposed equation was used to predict experimental data from the literature for the oxide fiber Nextel 720. An overall good fit was obtained with adjusted R^2 values of .76–.96 depending on the testing conditions and data scatter. Exponent m of 1.8 was calculated for Nextel 720 fibers at high stresses and 1473 K. This indicates that this fiber shows a change in main creep deformation mechanism when tested at higher stresses. Considering the determined exponent n of 3.0, the final power law exponent at high stresses is 5.4, which is similar to the values reported for Nextel 720 under such conditions.

Comparing the proposed equation with the well-known Arrhenius creep equation, both show an equally good fit considering the adjusted coefficient of variation. However, the Arrhenius equation predicts consistently higher values of strain rate, which tend to the maximum values of the data, while the proposed equation predicts lower strain rate values for the same data. In this regard, the proposed equation is more suitable to describe the creep rate over bigger stress ranges.

ACKNOWLEDGMENTS

The authors would like to thank the support of the Federal University of Santa Catarina/CTC.

Open access funding enabled and organized by Projekt DEAL.

ORCID

Renato Saint Martin Almeida  <https://orcid.org/0000-0002-6808-8665>

REFERENCES

- Armani CJ. Creep performance of oxide ceramic fiber materials at elevated temperature in air and in steam. [Doctor thesis]. Ohio: Air University, Department of the Air Force; 2011.
- Robinson RC, Smialek JL. SiC recession caused by SiO₂ scale volatility under combustion conditions: I, experimental results

- and empirical model. *J Am Ceram Soc.* 1999;82(7):1817–25. <https://doi.org/10.1111/J.1151-2916.1999.TB02004.X>
- Hackemann S, Flucht F, Braue W. Creep investigations of alumina-based all-oxide ceramic matrix composites. *Compos Part A Appl Sci Manuf.* 2010;41(12):1768–76. <https://doi.org/10.1016/j.compositesa.2010.08.012>
- Mattoni MA, Yang JY, Levi CG, Zok FW, Zawada LP. Effects of combustor rig exposure on a porous-matrix oxide composite. *Int J Appl Ceram Technol.* 2005;2(2):133–40. <https://doi.org/10.1111/J.1744-7402.2005.02015.X>
- Ruggles-Wrenn MB, Koutsoukos P, Baek SS. Effects of environment on creep behavior of two oxide/oxide ceramic-matrix composites at 1200°C. *J Mater Sci.* 2008;43(20):6734–46. <https://doi.org/10.1007/S10853-008-2784-X/FIGURES/15>
- Evans AG, Zok FW. The physics and mechanics of fibre-reinforced brittle matrix composites. *J Mater Sci.* 1994;29(15):3857–96. <https://doi.org/10.1007/BF00355946>
- Wilson DM, Lueneburg DC, Lieder SL. High temperature properties of nextel 610 and alumina-based nanocomposite fibers. *Ceram Eng Sci Proceed.* 1993;14(7–8):609–21. <https://doi.org/10.1002/9780470314180.CH87>
- Almeida RSM, Tushtev K, Clauß B, Grathwohl G, Rezwani K. Tensile and creep performance of a novel mullite fiber at high temperatures. *Compos Part A Appl Sci Manuf.* 2015;76:37–43. <https://doi.org/10.1016/j.compositesa.2015.05.013>
- Hay RS, Armani CJ, Ruggles-Wrenn MB, Fair GE. Creep mechanisms and microstructure evolution of Nextel™ 610 fiber in air and steam. *J Eur Ceram Soc.* 2014;34(10):2413–26. <https://doi.org/10.1016/J.JEURCERAMSOC.2014.01.032>
- Almeida RSM, Al-Qureshi HA, Tushtev K, Rezwani K. On the dimensional analysis for the creep rate prediction of ceramic fibers. *Ceram Int.* 2018;44(13):15924–28. <https://doi.org/10.1016/J.CERAMINT.2018.06.012>
- Armani CJ, Ruggles-Wrenn MB, Hay RS, Fair GE. Creep and microstructure of Nextel™ 720 fiber at elevated temperature in air and in steam. *Acta Mater.* 2013;61(16):6114–24. <https://doi.org/10.1016/j.actamat.2013.06.053>
- Khajuria A, Kumar R, Bedi R. Effect of boron addition on creep strain during impression creep of P91 steel. *J Mater Eng Perform.* 2019;28(7):4128–42. <https://doi.org/10.1007/s11665-019-04167-z>
- Khajuria A, Akhtar M, Bedi R, Kumar R, Ghosh M, Das CR, et al. Microstructural investigations on simulated intercritical heat-affected zone of boron modified P91-steel. *Mater Sci Technol.* 2020;36(13):1407–18. <https://doi.org/10.1080/02670836.2020.1784543>
- Khajuria A, Akhtar M, Bedi R, Kumar R, Ghosh M, Das CR, et al. Influence of boron on microstructure and mechanical properties of Gleeble simulated heat-affected zone in P91 steel. *Int J Pressure Vessels Piping.* 2020;188:104246. <https://doi.org/10.1016/j.ijpvp.2020.104246>
- Garg A, Belarbi M-O, Tounsi A, Li L, Singh A, Mukhopadhyay T. Predicting elemental stiffness matrix of FG nanoplates using Gaussian Process Regression based surrogate model in framework of layerwise model. *Eng Anal Bound Elem.* 2022;143:779–95. <https://doi.org/10.1016/j.enganabound.2022.08.001>
- Garg, A, Aggarwal P, Aggarwal Y, Belarbi M-O, Chalak HD, Tounsi A, et al. Machine learning models for predicting the compressive strength of concrete containing nano silica. *Comput Concrete.* 2022;30:33–42. [10.12989/cac.2022.30.1.033](https://doi.org/10.12989/cac.2022.30.1.033)

17. Sekban DM, Yaylacı EU, Özdemir ME, Yaylacı M, Tounsi A. Investigating formability behavior of friction stir-welded high-strength shipbuilding steel using experimental, finite element, and artificial neural network methods. *J Mater Eng Perform*. 2024. <https://doi.org/10.1007/s11665-024-09501-8>
18. Bridgman PW. *Dimensional analysis*, 2nd ed. Yale University Press; 1931.
19. Lemons DS. *A student's guide to dimensional analysis*, 1st ed. Cambridge University Press; 2017.
20. Buckingham E. On physically similar systems; illustrations of the use of dimensional equations. *Phys Rev*. 1914;4(4):345. <https://doi.org/10.1103/PhysRev.4.345>
21. Gálfi B-P, Száva I, Şova D, Vlase S. Thermal scaling of transient heat transfer in a round clad rod with modern dimensional analysis. *Mathematics*. 2021;9(16):1–24.
22. Langhaar HL. *Dimensional analysis and theory of models*, 1st ed. John Wiley & Son Ltd; 1951.
23. Almeida RSM, Bergmüller EL, Lührs H, Wendschuh M, Clauß B, Tushtev K, et al. Thermal exposure effects on the long-term behavior of a mullite fiber at high temperature. *J Am Ceram Soc*. 2017;100(9):4101–9. <https://doi.org/10.1111/JACE.14922>
24. Kobelev V. Some basic solutions for nonlinear creep. *Int J Solids Struct*. 2014;51(19–20):3372–81. <https://doi.org/10.1016/j.ijsolstr.2014.05.029>
25. Matthews FL, Rawlings RD. *Composite materials: engineering and science*. CRC Press; 1999.
26. Park SJ, Seo MK. Types of composites. *Interface Sci Technol*. 2011;18:501–629. <https://doi.org/10.1016/B978-0-12-375049-5.00007-4>
27. Chawla KK. *Composite materials science and engineering*. Springer; 1987.
28. Gonçalves DP, Melo FCL, Klein A, Al-Qureshi H. Analysis and investigation of ballistic impact on ceramic/metal composite armour. *Int J Mach Tools Manuf*. 2004;44:307–16. <https://doi.org/10.1016/j.ijmactools.2003.09.005>
29. Almeida RSM. Long-term behavior of polycrystalline oxide fibers at elevated temperatures. [Doctor thesis]. Bremen: University of Bremen, Production Engineering Department; 2017.
30. ASM International. In: Miracle DB and Donaldson SL, editors. *ASM Handbook Volume 21: Composites*. ASM International: Ohio; 2001.
31. Wilson D. Statistical tensile strength of Nextel™ 610 and Nextel™ 720 fibres. *J Mater Sci*. 1997;32(10):2535–42. <https://doi.org/10.1023/A:1018538030985>

How to cite this article: Berman RB, Almeida RSM, Azmah Hanim MA, dePieri ER, Al-Qureshi HA. Novel approach for predicting the creep behavior of ceramic fibers using dimensional analysis. *Int J Appl Ceram Technol*. 2024;1–8. <https://doi.org/10.1111/ijac.14876>